

MASS PROFILES OF GALAXY CLUSTER CORES:
IMPLICATIONS FOR STRUCTURE FORMATION AND
SELF-INTERACTING DARK MATTERJ.S. ARABADJIS¹ AND M.W. BAUTZ¹*Draft version November 14, 2018*

ABSTRACT

We present a spectroscopic deprojection analysis of a sample of ten relaxed galaxy clusters. We use an empirical F-test derived from a set of Markov Chain Monte Carlo simulations to determine if the core plasma in each cluster could contain multiple phases. We derive non-parametric baryon density and temperature profiles, and use these to construct total gravitating mass profiles. We compare these profiles with the standard halo parameterizations. We find central density slopes roughly consistent with the predictions of Λ CDM: $-1 \lesssim d \log(\rho) / d \log(r) \lesssim -2$. We constrain the core size of each cluster and, using the results of cosmological simulations as a calibrator, place an upper limit of $\sim 0.1 \text{ cm}^2 \text{ g}^{-1} = 0.2 \text{ b}(\text{GeV}/c^2)^{-1}$ (99% confidence) on the dark matter particle self-interaction cross section.

Subject headings: X-rays : galaxies: clusters — cosmology : dark matter

1. INTRODUCTION

The Λ CDM theory of cosmological structure formation – a cold dark matter (CDM) universe evolving under gravitation with a cosmological constant (Λ) – has been very successful in characterizing large scale structure on scales greater than $\sim 0.1 \text{ Mpc}$ (Mohr et al. 2000; Lahav et al. 2001; Spergel et al. 2003; Percival et al. 2003). However, Λ CDM makes three predictions which appear to conflict with observations. The first of these discrepancies is the “satellite problem” – the Milky Way contains at least an order of magnitude fewer satellites than simulations predict for a dark matter halo of its size (Kauffmann, White, & Guideroni 1993; Moore et al. 1999a; Klypin et al. 1999). The second is the “disk problem,” – disk galaxies produced in simulations contain too little mass and angular momentum (Navarro & Steinmetz 2000). The third is the “core problem” – galaxy-sized dark matter halos produced in simulations tend to have significantly steeper logarithmic density gradients in their cores than do observed structures.

The density profile of a dark matter halo formed through the hierarchical assembly of smaller structures is usually parameterized as a pair of power laws with a transition scale radius r_s (e.g. Jing & Suto (2002)),

$$\frac{\rho(r)}{\rho_0} = \frac{1}{(r/r_s)^\alpha (1+r/r_s)^{\gamma-\alpha}}, \quad (1)$$

with $\alpha = 1$ (Navarro, Frenk & White (1996, 1997); hereafter the “NFW” profile) or $\alpha = 1.5$ (Moore et al. (1999b); hereafter the “Moore” profile). While there is general agreement that $\gamma = 3$, rotation curves of low surface brightness (Burkert 1995; McGaugh & de Blok 1998) and spiral galaxies (Salucci & Burkert 2000; Gentile et al. 2000) and the fundamental plane of elliptical galaxies (Borriello et al. 2003) suggest that core density profiles are significantly flatter than Λ CDM, with $0 \geq \alpha \geq 1$.

¹ Center for Space Research, Massachusetts Institute of Technology, Cambridge, MA 02139; jsa@space.mit.edu, mwb@space.mit.edu

Reports of a core problem on galaxy cluster scales have been somewhat more controversial. Some lensing studies have found flat core profiles (Tyson, Kochanski & Dell’Antonio 1998; Smail et al. 2000) while others, making use of similar data sets, have not (Broadhurst et al. 2000; Shapiro & Iliev 2000). Most recently, Sand, Treu & Ellis (2002) and Sand et al. (2004) have found shallow ($\rho \sim r^{-0.5}$) cores in several clusters using a combination of radial and tangential strong lensing arcs in tandem with stellar velocity dispersion measurements.

The severity and cause of these discrepancies have been a subject of intense debate for nearly a decade. While observational limitations may play a role (Swaters, Madore & Trehella 2001), they are unlikely to be the sole cause in the majority of cases (Dalcanton & Bernstein 2000; Swaters, Madore & Trehella 2001; Swaters et al. 2003; Bolatto et al. 2003). Various explanations have been offered which can be ascribed to astrophysics or to particle physics. Most Λ CDM simulations evolve collisionless dark matter particles and baryons under the influence of gravitation only; final baryon distributions are usually determined according to prescription afterward. Thus, the disagreement between simulation and observation is either caused by neglected baryonic processes (astrophysics) which could act to flatten the baryon-dominated cores, or could be the result of neglected processes involving dark matter (particle physics).

It is certainly plausible that many of the problems on scales of $\sim 10 \text{ kpc}$ are the result of neglected baryon physics, if only because this is the scale at which star formation and the associated processes dominate the energy budget in galaxies. It seems less likely that discrepancies over the range 100-800 kpc, scales probed in the Sand et al. (2004) study, could have the same provenance. Thus if these measurements are correct they may require a significant revision of our understanding of structure formation and the behavior of dark matter. The literature already provides a plethora of alternative dark matter theories: self-

interacting dark matter (Spergel & Steinhardt 2000), warm dark matter (Hogan & Dalcanton 2000), annihilating dark matter (Kaplinghat, Knox & Turner 2000), scalar field dark matter (Goodman 2000; Hu & Peebles 2000), decaying dark matter (Cen 2001), and mirror matter (Mohapatra, Nussinov & Teplitz 2002; Foot 2004), to name several. Of these, self-interacting dark matter (SIDM) Spergel & Steinhardt (2000) has probably garnered the most attention, since with only one or two scattering events per particle over the age of the universe the cores of galaxies could be sufficiently softened to match observed galaxy profiles Davé et al. (2001) (hereafter DSSW). SIDM is also theoretically attractive in that it would produce softened cores on galaxy cluster scales Yoshida et al. (2000), potentially providing an explanation for the Sand et al. (2004) results.

The 10^8 K X-ray emitting cluster plasma provides an important alternative probe to gravitational lensing reconstructions of cluster mass profiles. Lensing studies, which measure projected mass, may preferentially select clusters with significant substructure along the line-of-sight (Cohn & Kochanek 2003). In addition, most lensing-derived masses are model-dependent reconstructions (e.g. Sand et al. (2004)). On the other hand, while X-ray mass determinations can utilize non-parametric spectroscopic deprojection, they are valid only if the hot plasma is in hydrostatic equilibrium. Those clusters for which this is most likely true usually display “cooling flow” emission which can alter the derived profile depending on how it is modelled (Allen (1998); Arabadjis, Bautz & Garmire (2002); Smith et al. (2004); Arabadjis, Bautz & Arabadjis (2004), hereafter ABA). Since these methods employ completely independent assumptions and potentially suffer from different systematic uncertainties, they constitute a powerful two-pronged attack on the core problem.

It has been argued (Markevitch et al. 2003) that the complex cluster surface brightness distributions revealed by Chandra throw the hydrostatic hypothesis into doubt. We take a more optimistic attitude, noting that we select clusters which are largely devoid of significant substructure. In addition, our method includes a diagnostic for clusters whose cores are not in hydrostatic equilibrium (see §2). We note that Kay et al. (2004) find that neglecting a kinematic pressure term from a hydrostatic analysis leads to errors in the determination of cluster masses of only $\sim 10\%$ for those whose cores contain cool plasma.

In this paper, we use X-ray imaging spectroscopy from the Chandra X-ray Observatory to constrain cluster mass profiles under the assumption of hydrostatic equilibrium. We briefly outline our mass profile extraction technique in §2. We then examine the core mass profiles of a sample of relaxed clusters and compare with the predictions of Λ CDM in §3. Finally we use these profiles to constrain the self-interaction cross section of dark matter particles in §4.

2. EXTRACTION OF MASS PROFILES

The spectroscopic deprojection and mass reconstruction technique we employ has been fully described elsewhere (Arabadjis, Bautz & Garmire 2002; Arabadjis, Bautz & Arabadjis 2004) so we only briefly summarize them here. Starting with a Chandra ACIS-S

or ACIS-I observation of a cluster, we process the data in the usual way², removing point sources and periods of high background. We divide the events into concentric annuli centered on the emission peak such that there are at least 1000-1500 source photons per annulus. We construct a model consisting of a set of concentric spherical shells whose inner and outer radii r_i and r_o correspond to the angular radii of the annuli in the data. Each shell is modelled as a thermal plasma at redshift z using the MEKAL model (Mewe, Gronenschild & van den Oord 1986; Mewe, Lemen & van den Oord 1986; Kaastra 1992; Liedahl, Osterheld & Goldstein 1995) within XSPEC (Arnaud 1996). Each plasma component is characterized by a temperature T and normalization K . (The metal abundances are set to 0.3 solar.) The normalization is related to the plasma density $\rho = \mu m_p n_H$ through the shell geometry,

$$K^{-1} = 10^{14} [4\pi D_A(1+z)]^2 \int_{r_i}^{r_o} n_e n_H r^2 dr \quad (2)$$

where D_A is the angular diameter distance of the cluster.

We test each cluster for the presence of a second (cooler) cospatial emission component in the core using an empirical F-test applied to a suite of 1000 Markov Chain Monte Carlo (MCMC) simulations per cluster. We use the MCMC significance S – defined as one minus the fraction of simulations which show an improvement in the model fitting as large as that shown by the data simply by chance – to decide whether a second core emission component is required, adopting a threshold of 0.99 for its inclusion (ABA).

We select clusters from the Chandra archive which display (i) a single peak in their X-ray emission and circular isophotes, and (ii) no obvious signs of merging activity or other asymmetry in their X-ray surface brightness distribution. Since these criteria are somewhat subjective, we further screen clusters in the sample according to the shape of their core mass profiles. Specifically, when deriving ensemble averages, we use only those clusters for which a power law is an acceptable fit ($\chi^2_r < 1.3$) to the core profile (the innermost 5 points in the profile, usually $r \lesssim 100$ kpc). We shall henceforth refer to these as the “relaxed core cluster” (RCC) subset. This prevents contamination of our sample from clusters which appear relaxed but whose irregular core mass profiles may belie the hydrostatic hypothesis. Seven of the 10 clusters in our original sample (ABA) are RCCs, though we include the remaining three objects for comparison in parts of this analysis. Table 1 lists the 10 clusters in the sample, their redshift, the treatment adopted for their core emission, the MCMC significance of the second component, and whether or not the cluster core is relaxed.

The model parameters, T_i , K ($i = 1, N$), and a Galactic absorption column N_{HI} are fit for simultaneously, and 2D confidence limits for each T_i, K_i (alternatively T_i, ρ_i) pair are calculated. The runs of temperature and density for each cluster are then used to calculate the total enclosed gravitating mass of the cluster M_r using the hydrostatic equation (Sarazin 1988):

$$M_r = 3.535 \times 10^{10} M_{\odot} \left(\frac{T}{1 \text{ keV}} \right) \left(\frac{r}{1 \text{ kpc}} \right) \left(-\frac{d \log T}{d \log r} - \frac{d \log \rho}{d \log r} \right) \quad (3)$$

² See <http://asc.harvard.edu/ciao/threads/all.html>

Statistical fluctuations in the temperature measurements can result in an unphysical mass determination, i.e. $M_r < 0$ or $dM/dr < 0$, over a limited range in r . To remedy this situation we *impose* the constraints $M_r > 0$ and $dM/dr > 0$ on the mass profile and allow the temperature and density of each shell to vary slightly in order to satisfy them. The degree to which these constraints are enforced is a free parameter (i.e. a weighting factor in a penalty function); if the variation in T , or less likely ρ , required to satisfy the constraints is excessive (e.g. $\Delta T/\sigma_T \gtrsim 1$) we conclude that one of our input assumptions, and therefore the mass profile, is suspect (ABA).

3. CORE PROFILES

In Figure 1 we show mass profiles (top) and cumulative power law slopes α (bottom) for all 10 sample clusters, with uniphase models at left and two-phase models at right. The exception to this is Hydra A, where we show only a uniphase model. Our attempts at fitting a second core component in this cluster resulted in its best-fit temperature matching that of the original component, consistent with David et al. (2001). For each cluster, the model with the higher MCMC F-test significance (ABA; see also Table 1) is indicated by the ‘preferred’ label.

The cumulative power law slope, plotted as filled squares, represents a power law fit to the profile as a function of the outermost point used in the fitting. The innermost value of α is duplicated at the minimum r value with an open square for clarity (except for Hydra A and A1795, whose core profiles are unphysical even with a significant weighting of the mass constraints term in the penalty function). Λ CDM predicts that α should asymptotically approach -1 (the NFW profile) or -1.5 (the Moore profile) as r decreases.

3.1. Uniphase versus two-phase

In general two-phase models have steeper central mass profiles than do uniphase models. This is so because the two-phase models allow the temperature of the hot component to remain roughly constant all the way in to spatial resolution limit. This augments the mass at each radius (see Equation 3), making M_r flatter in the center. Since $M_r \sim r^{\alpha+3}$, this implies a steeper density profile.

3.2. Comparison with previous studies

The profiles of power law slope show variation among the sample clusters, and in some cases between different plasma emission models (Figure 1). The core region of two of the clusters in our sample – Hydra A (McNamara et al. 2000; David et al. 2001), A1795 (Markevitch et al. 2001; Ettori et al. 2002), are known to be out of hydrostatic equilibrium. Figure 1 shows that the inferred mass profiles for these clusters are indeed irregular. Three of the most relaxed clusters in our sample – A2029, A1689 and MS2137 – have been modelled in detail in other studies, allowing us to compare mass profiles.

3.2.1. A2029

The inferred core profile of A2029 is sensitive to the assumed plasma model (Figure 1c). The uniphase model has a nearly flat core, whereas the two-phase core, which is preferred $> 99\%$ significance, is consistent with the

Moore profile. Confidence contours in α and the normalization M_0 (where $M_0 = M_r(1\text{Mpc})$) are shown in the upper left panels of Figure 2. The preferred two-phase model shows a core density that is even steeper than the Moore profile. These results differ from those of Lewis, Stocke & Buote (2002), who find no evidence for multiphase core plasma, based on a lack of significant reduction in the χ^2 value of their spectral fits, and Lewis, Buote & Stocke (2003) (hereafter LBS), who find that NFW provides a good fit to their mass profile. These discrepancies may be due in part to the specifics of the deprojection method used in each case. Our technique requires more photons per annulus than the “onion peeling” approach, essentially because it is non-parametric and global, to adequately constrain the temperature at each radius. We must therefore use larger regions for the extraction of spectra. The result is that we resolve temperature structure down to about 15 kpc, whereas LBS resolve it to ~ 3 kpc. In their model the plasma temperature drops a factor of two over this range, suggesting that perhaps the strong two-phase signature we see is due to a unresolved core temperature structure. We find strong evidence, however, for a second plasma component out to 34 kpc, well beyond our (and their) resolution limit, whereas LBS find none, so this cannot be the sole cause of the disparity. We note that Clarke et al. (2004) also find evidence for a second (cooler) emission component within $r < 40$ kpc.

In addition to spatial resolution, a fundamental difference between these two studies is the metric used to gauge the significance of the second component. LBS conclude that there is no evidence for multiphase plasma based on the lack of significant reduction in the χ^2 value of their fit (Lewis, Stocke & Buote 2002). Our method adopts the recommendation of Protassov et al. (2002), who have studied statistical tests used to compare pairs of models when one lies on a parameter-space boundary of the other (in our case, the normalization of the second component set to zero). They have found that the standard statistical tests can underestimate the signal in noisy data. In such cases one should use a statistical test performed on an empirical distribution derived from a large sample of data realizations which follow the complete parameter likelihood function. Following Protassov et al. (2002), our value for the significance of the second component is derived from the F distribution of a large MCMC sample (see §2). We believe therefore that our value for the core slope of A2029 is more reliable.

3.2.2. A1689

Andersson & Madejski (2004) used XMM-Newton data and the deprojection scheme of ABG to derive a core slope of -1.27 , which is consistent with our results. It should be noted that they find evidence for an asymmetry in the temperature structure of the plasma, and suggest that this could be due to a merger event. Our mass profile shows no evidence of a merger, although our model does show a temperature jump at this distance (ABA, Figure 5). It is not clear that this affects the value obtained for the core slope, however.

3.2.3. MS2137

Our profile for MS2137 is radically different from the strong gravitational lensing results of Sand, Treu & Ellis (2002). These authors use radial and tangential arcs in conjunction with the stellar velocity dispersion profile of the central galaxy to constrain the central density profile, finding $\alpha > -0.9$ at the 99% confidence limit. Our analysis yields $\alpha = -1.6 \pm 0.2$ (1σ), with $\alpha < -1.2$ at the 99% CL.

This discrepancy *cannot* be due to the difference between deriving a dark matter profile profile (Sand, Treu & Ellis 2002) and a total matter profile (this work). Baryons dominate the mass profile only up to 10 kpc (Sand et al. 2004); the innermost of our mass measurements is at $r \sim 20$ kpc. In addition, the Sand, Treu & Ellis (2002) analysis used a fixed NFW scale radius of 400 kpc; that is, 400 kpc marks the separation between the inner and outer power laws. Since all of our mass measurements are at radii smaller than this, our profile probes precisely the range where Sand, Treu & Ellis (2002) find a shallow inner profile.

We believe this is due to the nature of their lens model. Bartelmann & Meneghetti (2004) have shown that flat cores are indeed required for spherical and axisymmetric mass distributions, but if small deviations from axisymmetry are introduced (such as a mild ellipticity in the lensing potential, or a small external shear), these same systems are consistent with the cuspy profiles seen in simulations.

3.3. Central density slopes and Λ CDM

The confidence contours in Figure 2, shown for the RCC subset, show a range of values for the central density slope. This can be seen at the bottom of Figure 4; we find that $-1 \leq \alpha \leq -2$. This distribution appears somewhat steeper than CDM predictions (the gray band). Using symmetrized errors, we find a weighted mean of $\langle \alpha \rangle_w = -1.685 \pm 0.077$. The fact that this is marginally steeper than the CDM band is not surprising, since the contraction of cooling baryons is expected to deepen the central cluster potential, and thus steepen the central density profile (Hennawi & Ostriker (2002); Gnedin et al. (2004); but see also Loeb & Peebles (2003)). None of the clusters in the sample is consistent with the flat or nearly-flat cores found by Sand et al. (2004). We note, however, that only one cluster – MS2137 – appears in both samples.

One can interpret these results in at least two ways. It is thought that baryonic processes could act to steepen the mass profile as energy is removed from the cluster core via relaxation and radiative cooling effects. The adiabatic contraction of the core baryons deepens the potential well, causing the dark matter profile to steepen (Hennawi & Ostriker 2002). Another possibility is that merger tree hysteresis in the formation and evolution of the cluster, distinct from baryonic physics, dictates the current value of slope of the core dark matter profile (Ma & de Boylan-Kolchin 2004). The question of which influence – adiabatic contraction or accretion hysteresis – is dominant in setting the core profile, and the degree to which heating from a central AGN may play a role (Omma et al. 2004; Omma & Binney 2004), may remain unsettled until numerical experiments are able to self-consistently simulate the gas dynamics and cooling in conjunction with the gravitational evolution.

4. CORE PROFILES AND SIDM

We find that our mass profiles are adequately described by the theory of structure formation in an Λ CDM universe, so we can use them to bound the strength of the dark matter particle-particle self-interaction. Spergel & Steinhardt (2000) originally proposed SIDM as a solution to the core problem on galaxy scales. DSSW used numerical experiments to show that a self-interaction cross section σ_{DM} in the range 0.5 to $5 \text{ cm}^2 \text{ g}^{-1}$ (~ 1 to $10 \text{ b}(\text{GeV}/c^2)^{-1}$) provided the requisite flattening for galaxy-sized dark matter haloes. As they have noted, a cross section of this size is probably inconsistent with the distribution of halo shapes in cosmological simulations (see also Yoshida et al. (2000)). They also point out the difficulty inherent in core profile comparisons between simulations and observations, noting the indeterminate effect of baryon physics.

Arabadjis, Bautz & Garmire (2002) showed that the mass profile for the relaxed cluster MS1358 was inconsistent with $\sigma_{\text{DM}} > 0.1 \text{ cm}^2 \text{ g}^{-1}$. This was based on a comparison with the Yoshida et al. (2000) simulations which provided an informal relationship between cluster core size and self-interaction cross section. Markevitch et al. (2003) noted the need for a sample of clusters to place a robust limit on the cross section, and derived a less restrictive limit of $1 \text{ cm}^2 \text{ g}^{-1}$ based on a small offset between the weak lensing and X-ray peaks of a supersonic subcluster in 1E 0657-56.

In order to gauge the dark matter self-interaction strength, we determine the maximum core size of each cluster in the sample. Although we see no evidence for a constant density core in any cluster, we calculate the size of such an unresolved core that would be consistent with the data. We model each core as a softened isothermal profile sphere (Arabadjis, Bautz & Garmire 2002), fitting for its size and density normalization:

$$\rho(r) = \frac{\sigma^2}{2\pi G(r^2 + r_c^2)} \quad (4)$$

where σ is the (constant) 1D velocity dispersion and r_c is the core radius. Since our profiles are determined in cumulative mass, rather than density, we fit for r_c and M_0 using $M_r = M_0(x - \tan^{-1}x)$, where $x = r/r_c$ and the mass scale $M_0 = 2\sigma^2 r_c^2/G$.

To limit the variance of the fitted parameters which are due to a non-hydrostatic core, we do the analysis only for the RCC subset (see Table 1). Confidence contours in core radius and mass scale are shown in Figure 3. A similar relationship obtains between core radius and two-phase plasma to that found for core slope: two-phase emission models result in smaller core sizes or upper limits. As in the case of core slope, the effect is most pronounced in A2029. Thus the limits derived from uniphase core models can be considered to be conservative estimates.

The core radii of the RCC subset are shown at the top in Figure 4. (The corresponding core slopes for the same clusters are shown below.) The dashed lines show core sizes expected for three values of the dark matter self-interaction cross section (Yoshida et al. 2000). The DSSW cross section required to solve the core problem – 0.5 to $5 \text{ cm}^2 \text{ g}^{-1}$ – is clearly ruled out. Using symmetrized errors, the weighted mean core size is

$\langle r_c \rangle = 35.9 \pm 15.4$ kpc, corresponding to self-interaction cross section $\sigma_{DM} \ll 0.1 \text{ cm}^2 \text{ g}^{-1}$. We place a 99% upper limit of 65 kpc on the cluster core size, corresponding to just under $0.1 \text{ cm}^2 \text{ g}^{-1}$.

A few caveats must be mentioned here. The first is that this upper limit is derived from a calibration with simulations which did not include the effects of baryon physics in the core evolution. Presumably the adiabatic contraction of the core from radiative losses could counteract some effects of dark matter self-interaction, and could be consistent with the observations, provided that the contraction timescale is comparable to the mean time between dark matter particle scatterings (to prevent cooling-induced core collapse), and that the self-interaction is not so vigorous that gravitational core collapse proceeds in a Hubble time. However it is not clear that the baryons only act to hasten core contraction. Astrophysical processes associated with AGN or star formation, such as jet/ICM interactions, supernovae and stellar winds, may be required to match observables such as the “excess entropy” in groups and clusters Frenk (2002), although the issue of feedback is beyond the scope of this paper.

A second point is that the self-interaction cross sections in the calibration simulations (Yoshida et al. 2000) were assumed to be velocity independent. DSSW pointed out that a cross section which scaled as v^{-1} might ameliorate the discrepancies between SIDM cluster simulations and observations. A functional dependence such as $\sigma_{DM} = \sigma_0(v/v_0)^{-\gamma}$ might reduce the effects of self-interaction on cluster scales, although early results are not promising (N. Yoshida, private communication).

Finally, if the properties of the core are in fact governed by cluster accretion hysteresis (Ma & de Boylan-Kolchin 2004), measurements of cluster core properties will probably tell us little until we have a sufficiently large observational sample that we can explore the relevant physics through statistical analyses.

5. SUMMARY

We have presented an analysis of 10 galaxy clusters observed with the Chandra X-ray Observatory. We have carefully modelled their cores, utilizing a second plasma component where required. We have derived mass profiles for each of them, and for the RCC subset we find that Λ CDM provides an adequate description of their cores. We have placed upper limits on the size of any constant density core in each cluster, and derive a 99% upper limit of just under $0.1 \text{ cm}^2 \text{ g}^{-1} = 0.2 \text{ b}(\text{GeV}/\text{c}^2)^{-1}$ for the dark matter self-interaction cross section.

REFERENCES

Allen, S.W. 1998, MNRAS, 296, 392

Andersson, K.E. & Madejski, G.M. 2004, ApJ, 607, 190

Arabadjis, J.S., Bautz, M.W. & Arabadjis, G. 2004, ApJ, in press (astro-ph/0305547)

Arabadjis, J.S., Bautz, M.W. & Garmire, G.P. 2002, ApJ, 572, 78

Arnaud, K.A. 1996, *Astronomical Data Analysis Software and Systems V*, George H. Jacoby & Jeannette Barnes, eds., ASP Conf. Ser., 101, 17

Bartelmann, M. & Meneghetti, M. 2004, A&A, 418, 413

Bolatto, A.D., Simon, J.D., Leroy, A. & Blitz, L. 2003, in IAU Symposium 220, *Dark Matter in Galaxies*, eds. S. Ryder et al. (astro-ph/0311259)

Borriello, A., Salucci, P. & Danese, L. 2003, ApJ, 341, 1109

Broadhurst, T., Huang, X., Frye, B., & Ellis, R. 2000, ApJ, 534, 15

Burkert, A. 1995, ApJ, 447, L25

Cen, R. 2001, ApJL, 546, L77

Clarke, T.E., Blanton, E.L. & Sarazin, C.L. 2004, ApJ, in press (astro-ph/0408068)

Cohn, J.D. & Kochanek, C.S. 2003, astro-ph/0306171

Dalcanton, J.J. & Bernstein, R.A. 2000, in *XVth IAP Meeting, Dynamics of Galaxies: From the Early Universe to the Present*, eds. F. Combes, G.A. Mamon & V. Charmandaris

Davé, R., Spergel, D.N., Steinhardt, P.J. & Wandelt, D. 2001, ApJ, 547, 574 [DSSW]

David, L.P., Nulsen, P.E.J., McNamara, B.R., Forman, W., Jones, C., Ponman, T., Robertson, B. & Wise, M. 2001, ApJ, 557, 546

Ettori, S., Fabian, A.C., Allen, S.W. & Johnstone, R.M. 2002, MNRAS, 331, 635

Foot, R. 2004, Phys. Rev. D, 69, 036001

Frenk, C.S. 2002, *Phi. Trans. Roy. Soc.*, 300, 1277

Gentile, G., Salucci, P., Klein, U., Vergani, D. & Kalberla, P. 2004, MNRAS, in press (astro-ph/0403154)

Gnedin, O.Y., Kravtsov, A.V., Klypin, A.A. & Daisuke, N. 2004, ApJ, submitted (astro-ph/0406247)

Goodman, J. 2000, New Astron., 5, 103
adiabatic contraction of core baryons / adiabatic compression of DM halo

Hennawi, J.F. & Ostriker, J.P. 2002, ApJ, 572, 41

Hogan, C.J. & Dalcanton, J.J. 2000, Phys. Rev. D, 62, 063511

Hu, W. & Peebles, P.J.E. 2000, ApJ, 528, 61
generalized broken power-law density profile

Jing, Y.P. & Suto, Y. 2002, ApJ, 574, 538

Kaplinghat, M., Knox, L. & Turner, M.S. 2000, Phys. Rev. Lett., 85, 3335

Kaastra, J.S. 1992, *An X-Ray Spectral Code for Optically Thin Plasmas*, Internal SRON-Leiden Report, version 2.0.

Kauffmann, G., White, S.D.M. & Guiderdoni, B. 1993, MNRAS, 264, 201

Kay, S.T., Thomas, P.A., Jenkins, A. & Pearce, F.R. 2004, MNRAS, submitted (astro-ph/0407058)

Klypin, A.A., Kravtsov, A.V., Valenzuela, O. & Prada, F. 1999, ApJ, k522, 82

Lahav, O., Bridle, S.L., Percival, W.J., Peacock, J.A., Efstathiou, G., Baugh, C.M., Bland-Hawthorn, J., Bridges, T., Cannon, R., Cole, S., Colless, M., Collins, C., Couch, W., Dalton, G., de Propris, R., Driver, S.P., Ellis, R.S., Frenk, C.S., Glazebrook, K., Jackson, C., Lewis, I., Lumsden, S., Maddox, S., Moody, S., Norberg, P., Peterson, B.A., Sutherland, W., & Taylor, K. 2001, MNRAS, 333, 961

Lewis, A.D., Buote, D.A. & Stocke, J.T. 2002, ApJ, 586, 135 [LBS]

Lewis, A.D., Stocke, J.T. & Buote 2002, ApJL, 573, L13

Liedahl, D.A., Osterheld, A.L. & Goldstein, W.H. 1995, ApJL, 438, L115

Loeb, A. & Peebles, P.J.E. 2003, ApJ, 589, 29

Ma, C-P. & Boylan-Kolchin, M. 2004, astro-ph/0403102

Markevitch, M., Gonzales, A.H., Clowie, D., Vikhlinin, A., Forman, W., Jones, C., Marray, S. & Tucker, W. 2003, ApJ, in press (astro-ph/0403102)

Markevitch, M., Vikhlinin, A., & Forman, W. 2002, *Matter and Energy in Clusters of Galaxies*, S. Bowyer & C.-Y. Hwang, eds., ASP Conf. Ser., 301, 37

Markevitch, M., Vikhlinin, A. & Mazzotta, P. 2001, ApJ, 562, L153

McGaugh, S.S. & de Blok, W.J.G. 1998, ApJ, 499, 41

Mewe, R., Gronenschild, E.H.B.M. & van den Oord, G.H.J. 1985, A&AS, 62, 197

Mewe, R., Lemen, J.R. & van den Oord, G.H.J. 1986, A&AS, 65, 511

McNamara, B.R., Wise, M., Nulsen, P.E.J., David, L.P., Sarazin, C.L., Bautz, M., Markevitch, M., Vikhlinin, A., Forman, W.R., Jones, C. & Harris, D.E. 2000, ApJL, 534, L135

Mohapatra, R.N., Nussinov, S. & Teplitz, V.L. 2002, Phys. Rev. D, 66, 063002

Mohr, J.J., Reese, E.D., Ellingson, E., Lewis, A.D. & Evrard, A.E. 2000, ApJ, 544, 109

Moore, B., Ghigna, S., Governato, F., Lake, G., Quinn, T., Stadel, J., & Tozzi, P. 1999a, ApJL, 524, L19

Moore, B., Quinn, T., Governato, F., Stadel, J. & Lake, G. 1999, MNRAS, 310, 1147

Navarro, J.F., Frenk, C.S. & White, S.D.M. 1997, ApJ, 462, 563

Navarro, J.F., Frenk, C.S. & White, S.D.M. 1997, ApJ, 490, 493

Navarro, J.F. & Steinmetz, M. 2000, ApJ, 528, 607

Omra, H., Binney, J. 2004, MNRAS, 348, 1105

Omra, H. & Binney, J. 2004, MNRAS, 350, L13

Percival, W.J., Sutherland, W., Peacock, J.A., Baugh, C.M., Bland-Hawthorn, J., Bridges, T., Cannon, R., Cole, S., Colless, M., Collins, C., Couch, W., Dalton, G., De Propris, R., Driver, S.P., Efstathiou, G., Ellis, R.S., Frenk, C.S., Glazebrook, K., Jackson, C., Lahav, O., Lewis, I., Lumsden, S., Maddox, S., Moody, S., Norberg, P., Peterson, B.A. & Taylor, K. 2002, MNRAS, 337, 1068

Protassov, R., van Dyk, D.A., Connors, A., Kashyap, V.L. & Siemiginowska, A. 2002, ApJ, 571, 545

Salucci, P. & Burkert, A. 2000, ApJL, 547, L9

Sand, D.J., Treu, T., Smith, G.P. & Ellis, R.S. 2004, ApJ, in press (astro-ph/0309465)

Sand, D.J., Treu, T. & Ellis, R.S. 2002, ApJL, 574, L129

Sarazin, C.L. 1988, *X-ray Emission from Clusters of Galaxies*, Cambridge Astrophysics Series, Cambridge: Cambridge University Press

Shapiro, P.R. & Iliev, I.T., 2000, ApJL, 542, L1

Smail, I., Ellis, R., Richehett, M.J. & Edge, A.C. 1995, MNRAS, 273, 277

Smith, G.P., Kneib, J.-P., Smail, I., Mazzotta, P., Ebeling, H. & Czoske, O. 2004, MNRAS, submitted

Spergel, D.N., Verde, L., Peiris, H.V., Komatsu, E., Nolta, M.R., Bennett, C.L., Halpern, M., Hishaw, G., Jarosik, N., Kogut, A., Limon, M., Meyer, S.S., Page, L., Tucker, G.S., Weiland, J.L., Wollack, E. & Wright, E.L. 2003, ApJS, 148, 175

Spergel, D.N. & Steinhardt, P.J. 2000, Phys. Rev. Lett., 84, 17

Swaters, R.A., Madore, B.F., van den Bosch, F.C. & Balcells, M. 2003, ApJ, 583, 732

R.A. Swaters, Verheijen, M. A. W., Bershady, M.A. & Andersen, D.R. 2003, in IAU Symposium 220, *Dark Matter in Galaxies*, eds. S. Ryder et al. (astro-ph/0311480)

Swaters, R.A., Madore, B.F. & Trewella, M. 2000, ApJ, 531, L107

Tyson, J.A., Kochanski, G.P. & Dell'Antonio, I.P. 1998, ApJ, 498, L107

Yoshida, N., Springel, V., White, S.D.M., & Tormen, G., 2001, ApJL, 544, L87

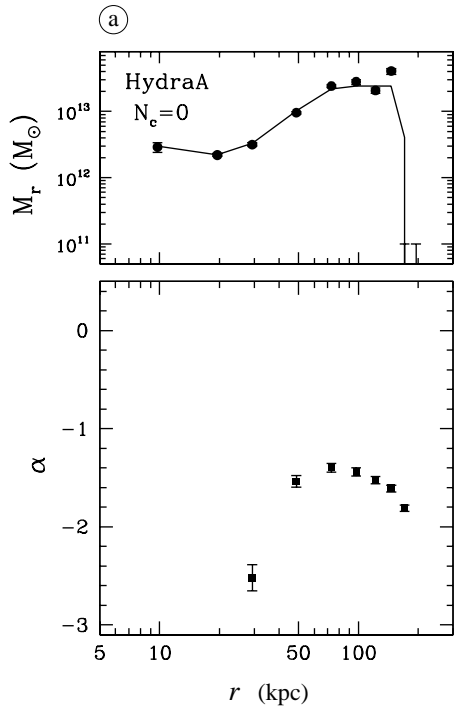
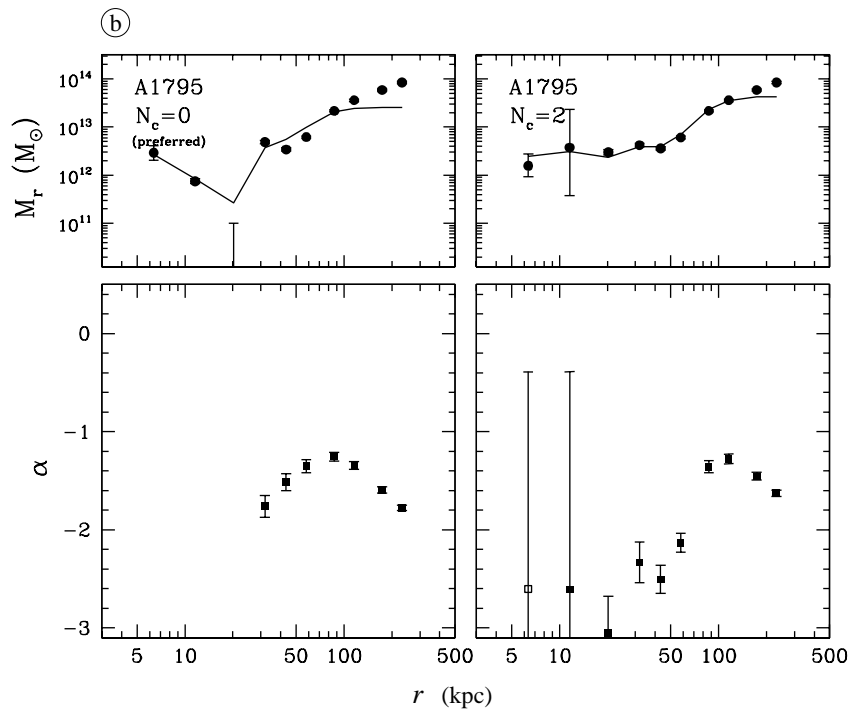
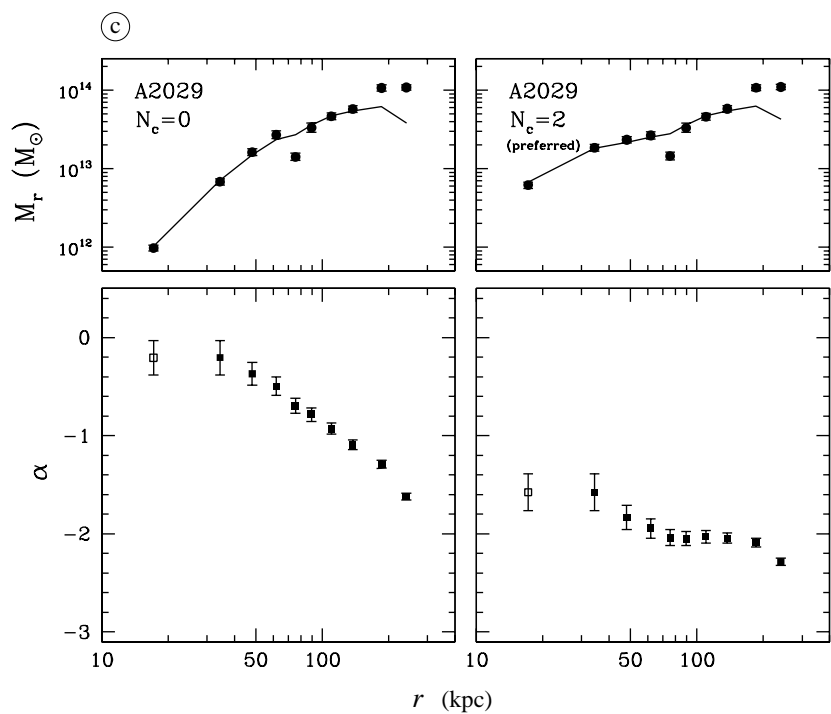
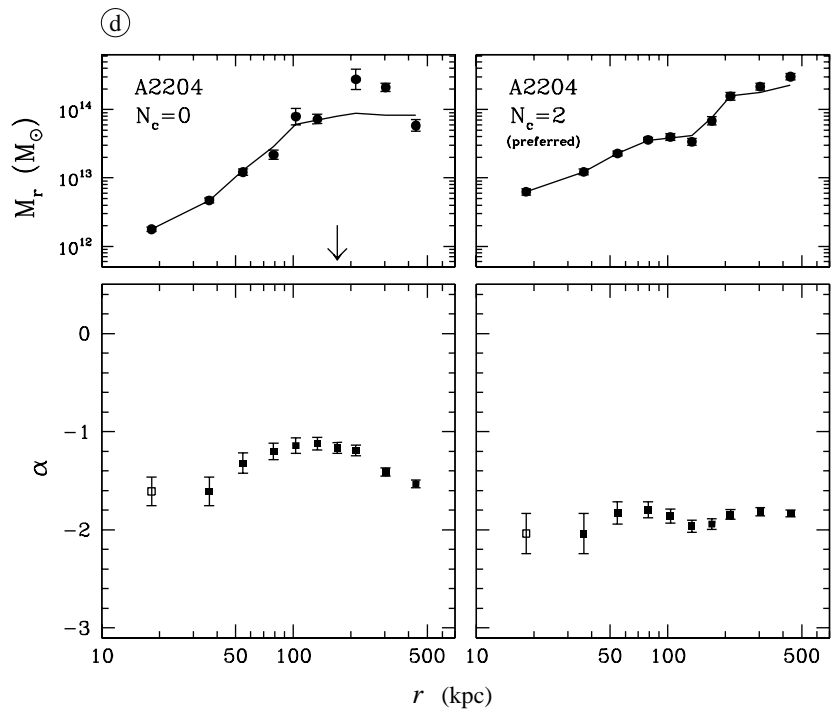
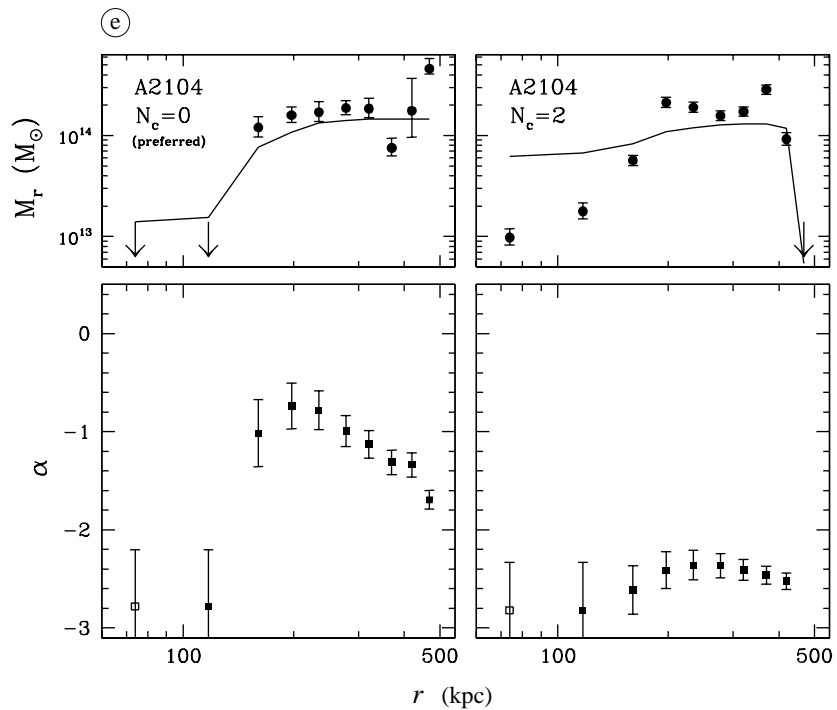


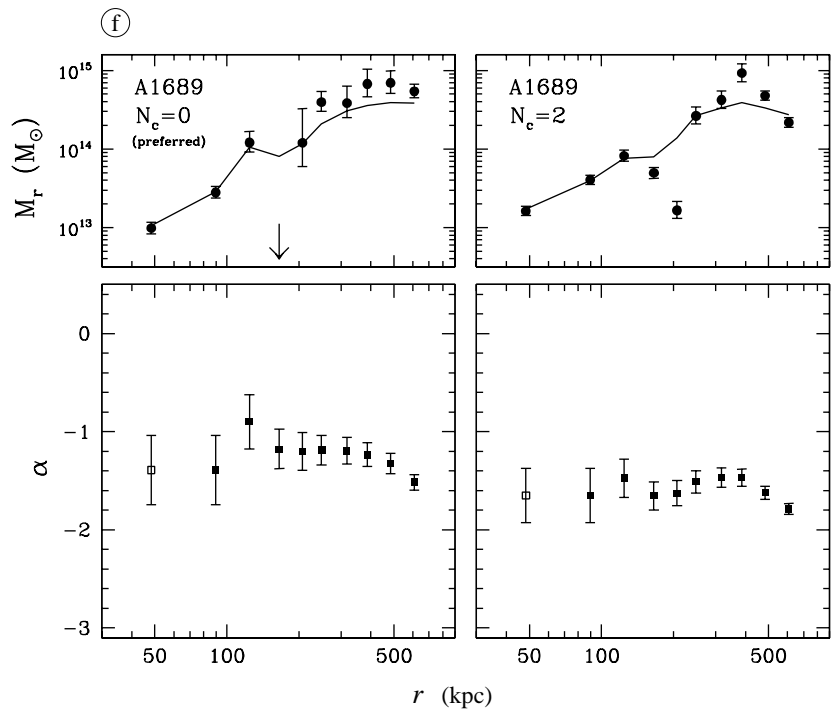
FIG. 1.— Mass profiles (top) and core power law slopes (bottom) of each cluster in the sample. We show profiles for uniphase (left) and two-phase (right) models of the core plasma (except for Hydra A; see text). The ‘preferred’ label appears on the model with the higher MCMC significance.

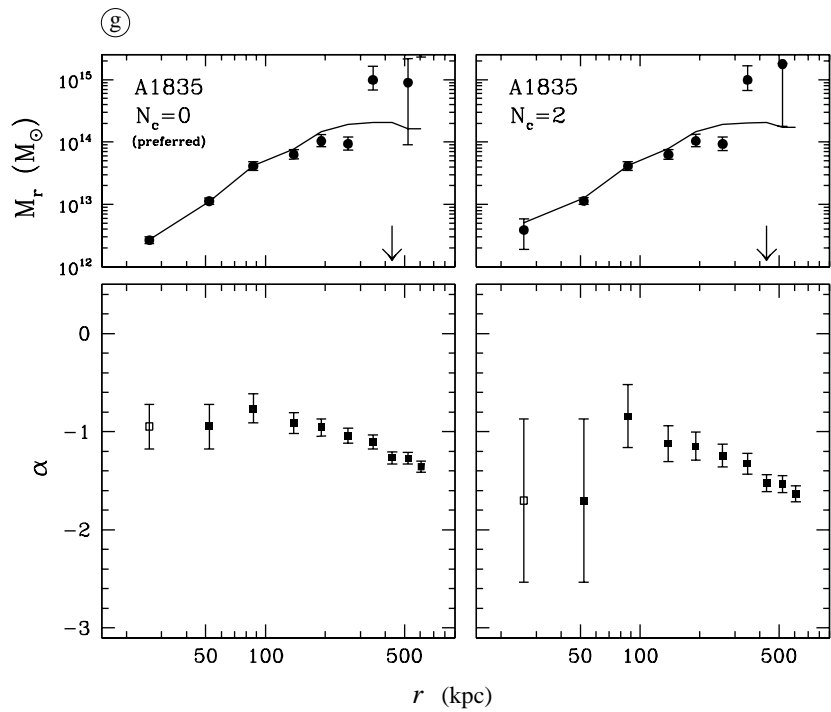


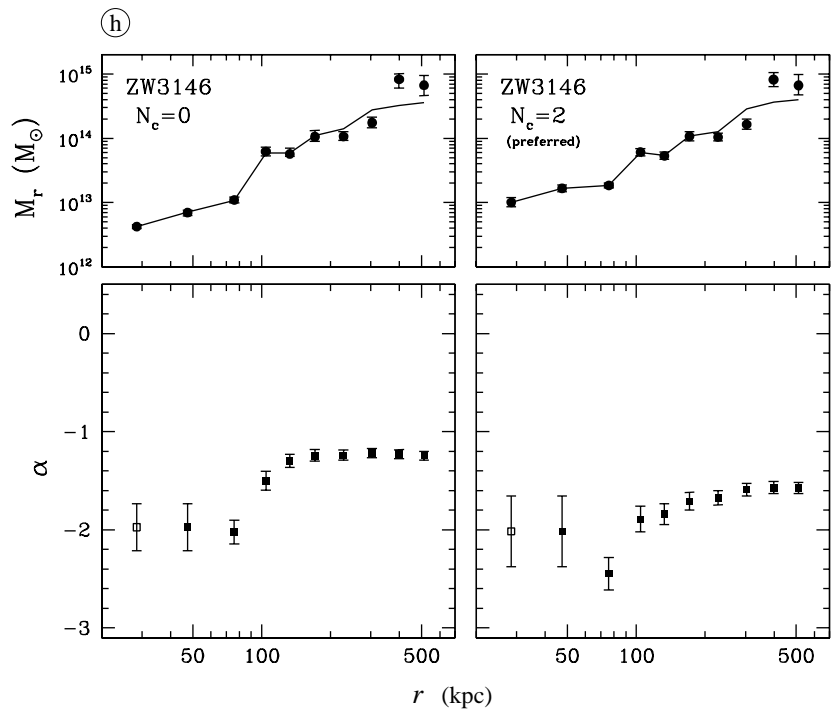


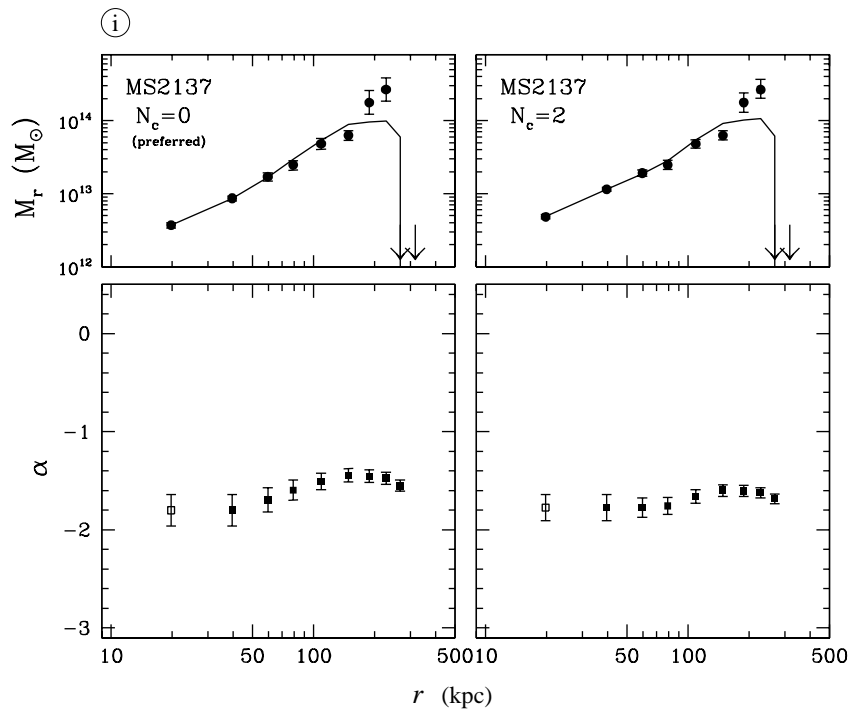


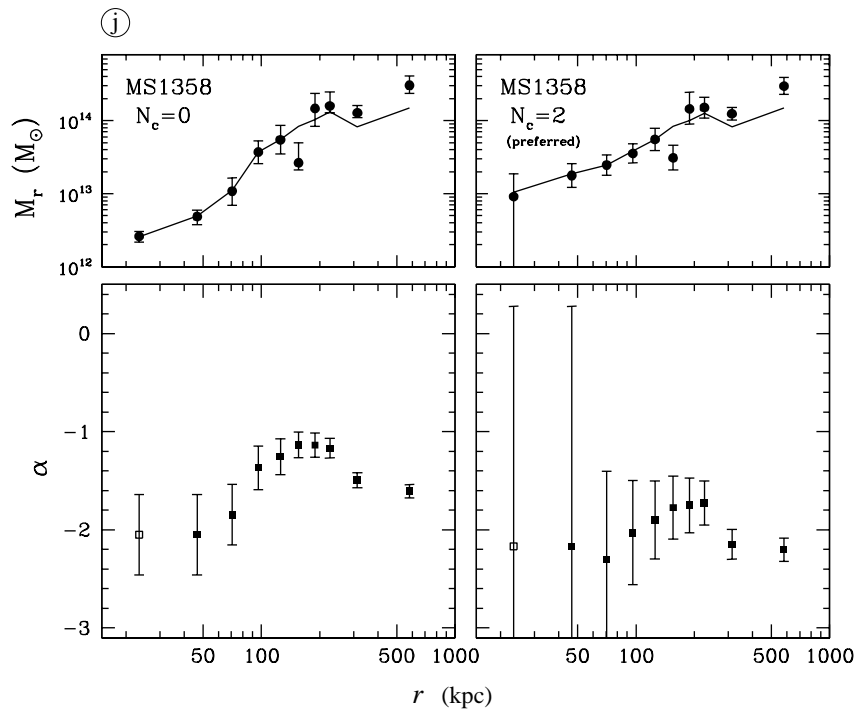












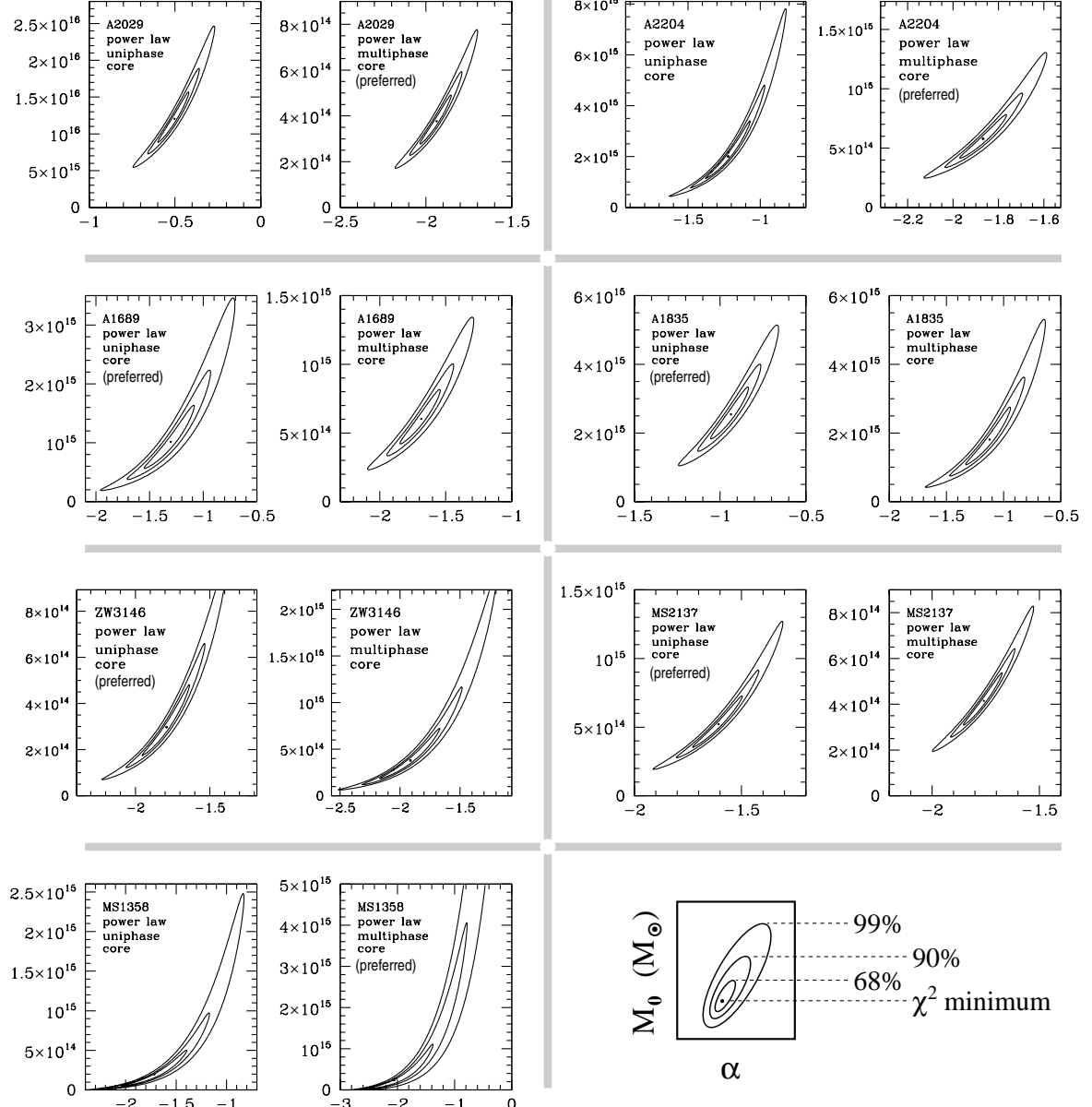


FIG. 2.— Confidence contours of power law fits to the cores of the RCC subset. The left/right plot in each pair is for uniphase/two-phase models of the core plasma. The model with the higher MCMC F-test significance is labeled ‘preferred’.

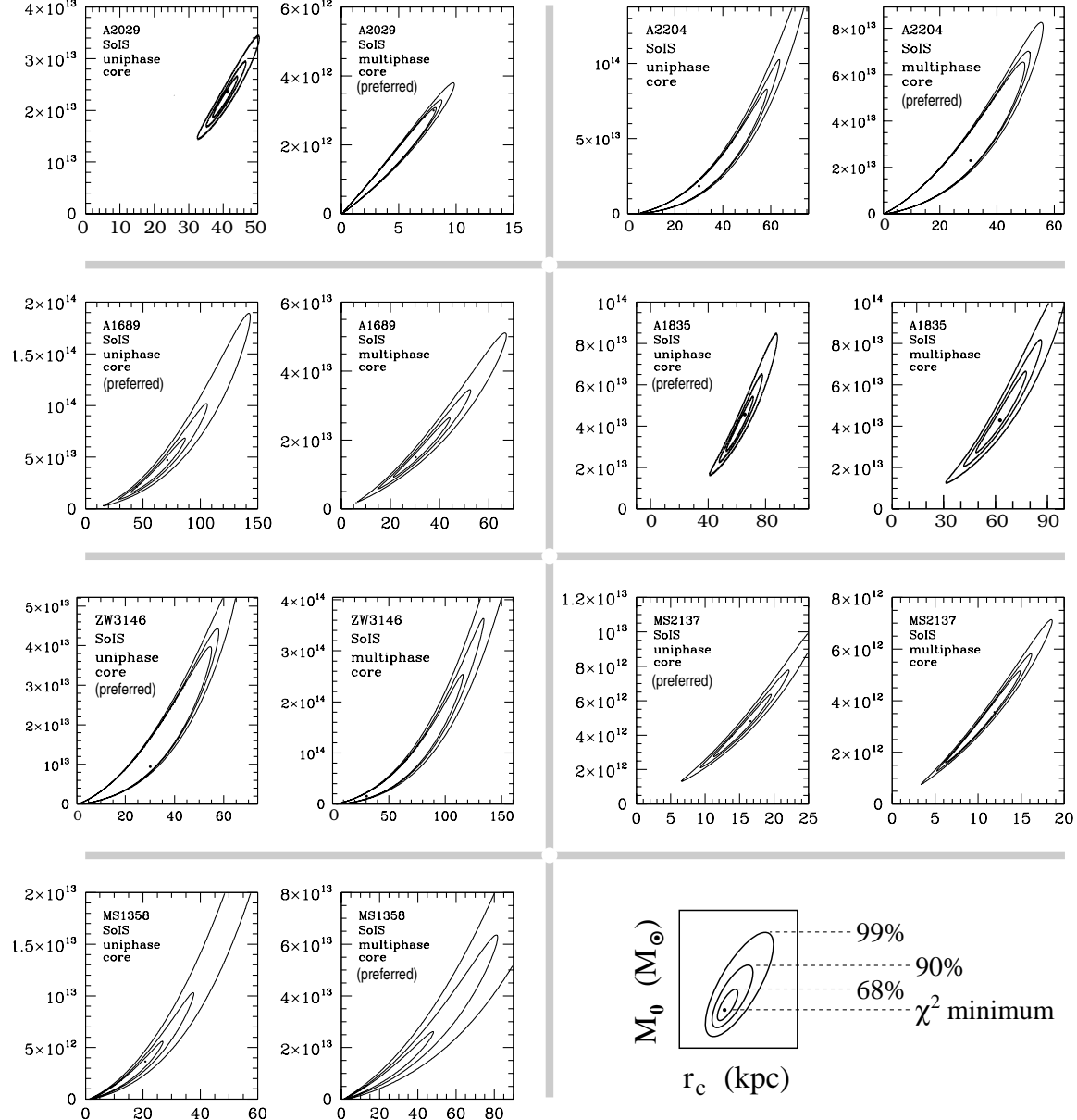


FIG. 3.— Confidence contours of softened isothermal sphere fits to the cores of the RCC subset. The left/right plot in each pair is for uniphase/two-phase models of the core plasma. The model with the higher MCMC F-test significance is labeled ‘preferred’.

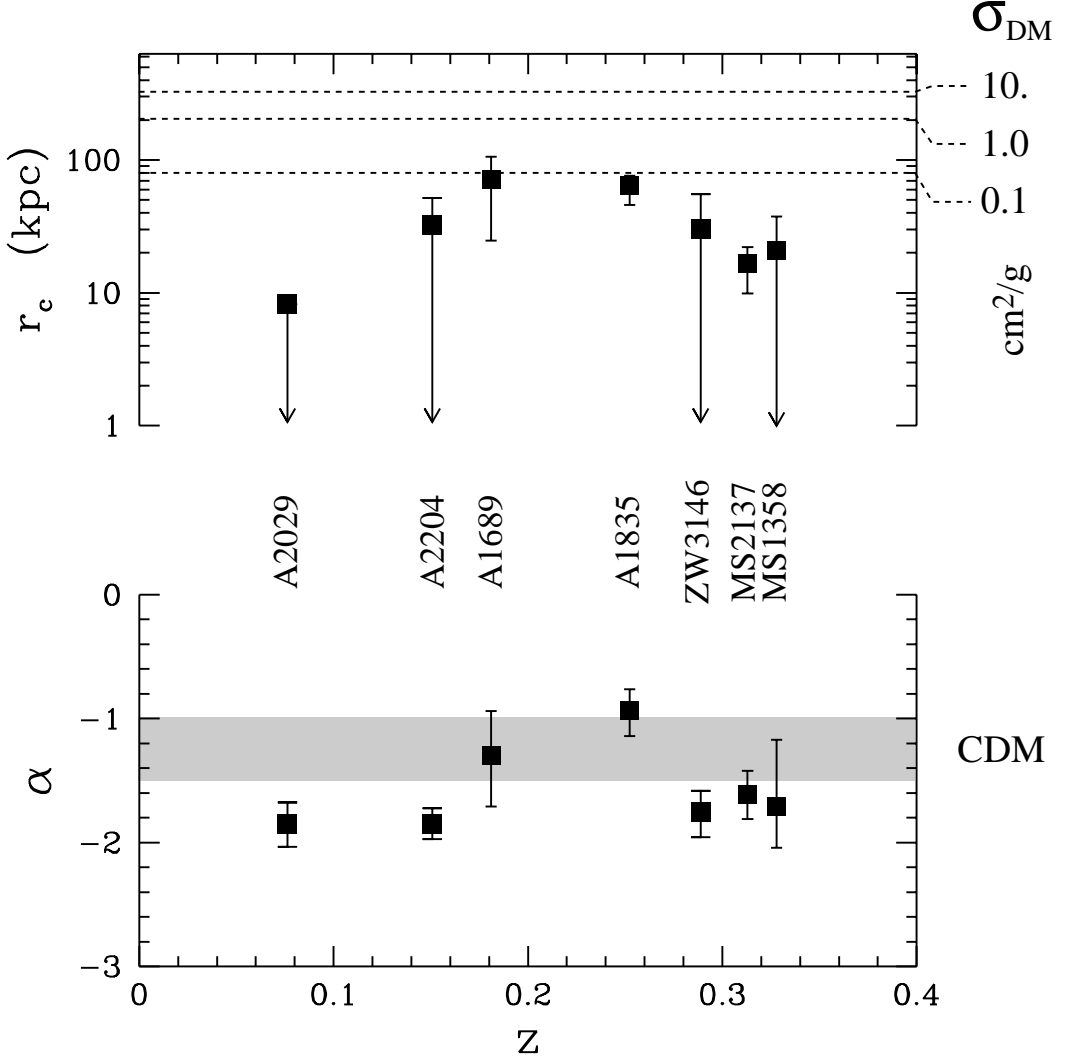


FIG. 4.— Summary of the softened isothermal sphere core radii (top) and power law slopes (bottom) for fits to the RCC subset. The relation between the self-interaction cross section of dark matter particles σ_{DM} and the cluster core radius r_c , taken from Yoshida et al. (2000), is denoted by dashed lines. The inner slope predictions of numerical CDM experiments is shown by a gray band bracketed by the values from Navarro, Frenk & White (1996, 1997) at $\alpha = -1$ and Moore et al. (1999b) at $\alpha = -1.5$.

TABLE 1
 GALAXY CLUSTER SAMPLE

cluster	z	core plasma	<i>S</i>	RCC?
Hydra A	0.0522	uniphase	—	no
Abell 1795	0.0631	uniphase	0.823	no
Abell 2029	0.0765	two-phase	0.998	yes
Abell 2204	0.1523	two-phase	0.999	yes
Abell 2104	0.1554	uniphase	0.661	no
Abell 1689	0.181	uniphase	0.342	yes
Abell 1835	0.2523	uniphase	0.483	yes
ZwCl 3146	0.2906	two-phase	0.989	yes
EMSS 2137–2353	0.313	uniphase	0.271	yes
EMSS 1358+6245	0.328	two-phase	0.987	yes